Published in final edited form as:
Biochemistry. 2013 August 6; 52(31): . doi:10.1021/bi400797c.

Unexpected reactivity of 2-fluorolinalyl diphosphate in the active site of crystalline 2-methylisoborneol synthase

Mustafa Köksal[†,‡], **Wayne K. W. Chou**[§], **David E. Cane**[§,*], and **David W. Christianson**[†,*]

[†]Roy and Diana Vagelos Laboratories, Department of Chemistry, University of Pennsylvania, 231 South 34th Street, Philadelphia, PA 19104-6323 USA

[§]Department of Chemistry, Brown University, Box H, Providence, RI 02912-9108 USA

Abstract

The crystal structure of 2-methylisoborneol synthase (MIBS) from *Streptomyces coelicolor* A3(2) has been determined in its unliganded state and in complex with 2 Mg^{2+} ions and *cis*-2-fluorogeranyl diphosphate at 1.85 Å and 2.00 Å resolution, respectively. Under normal circumstances, MIBS catalyzes the cyclization of the naturally-occurring, non-canonical 11-carbon isoprenoid substrate, 2-methylgeranyl diphosphate, which first undergoes an ionization-isomerization-ionization sequence through the tertiary diphosphate intermediate 2-methyllinalyl diphosphate to enable subsequent cyclization chemistry. MIBS does not exhibit catalytic activity with 2-fluorogeranyl diphosphate, and we recently reported the crystal structure of MIBS complexed with this unreactive substrate analogue [Köksal, M., Chou, W. K. W., Cane, D. E., Christianson, D. W. (2012) *Biochemistry 51*, 3011–3020]. However, cocrystallization of MIBS with the fluorinated analogue of the tertiary allylic diphosphate intermediate, 2-fluorolinalyl diphosphate, reveals unexpected reactivity for the intermediate analogue and yields the crystal structure of the complex with the primary allylic diphosphate, 2-fluoroneryl diphosphate. Comparison with the structure of the unliganded enzyme reveals that the crystalline enzyme active site remains partially open, presumably due to the binding of only 2 Mg^{2+} ions. Assays in solution indicate that MIBS catalyzes the generation of (1*R*)-(+)-camphor from the substrate 2-fluorolinalyl diphosphate, suggesting that both 2-fluorolinalyl diphosphate and 2-methyllinalyl diphosphate follow the identical cyclization mechanism leading to 2-substituted isoborneol products; however, the initially generated 2-fluoroisoborneol cyclization product is unstable and undergoes elimination of hydrogen fluoride to yield (1*R*)-(+)-camphor.

Terpenes, also known as terpenoids or isoprenoids, comprise a structurally and stereochemically diverse family of natural products that contains more than 70,000 members (Dictionary of Natural Products: http://dnp.chemnetbase.com).[1–6] The exquisite chemodiversity of these natural products is particularly impressive because their

[*]Authors to whom correspondence should be addressed: D.W.C.: Tel.: (215) 898-5714; chris@sas.upenn.edu. D.E.C.: Tel: (401) 863-3588; david_cane@brown.edu.
[‡]Current Address: Department of Molecular Biology and Genetics, Izmir Institute of Technology, Urla, Izmir, 35430 Turkey

Accession Codes

The atomic coordinates and the crystallographic structure factors of unliganded 2-methylisoborneol synthase from *Streptomyces coelicolor* and its complex with $Mg^{2+}{}_2$-2-fluoroneryl diphosphate (2-fluoro-*cis*-geranyl diphosphate) generated *in situ* from 2-fluorolinalyl diphosphate have been deposited in the Protein Data Bank (www.rcsb.org) with accession codes 4LA5 and 4LA6, respectively.

The authors declare no competing financial interests.

Supporting Information

NMR spectra of 2FLPP, and GC-MS data for enzymatically generated compounds and standards. This material is available free of charge via the Internet at http://pubs.acs.org.

hydrocarbon skeletons are typically derived from one of just a few isoprenoid precursors containing multiple 5-carbon isoprenoid units connected in head-to-tail fashion, e.g., the monoterpene (C_{10}) geranyl diphosphate, the sesquiterpene (C_{15}) farnesyl diphosphate, or the diterpene (C_{20}) geranylgeranyl diphosphate. The metal ion-dependent enzymes that catalyze the cyclization of these isoprenoid diphosphate substrates are designated class I terpenoid cyclases.[7] These enzymes initiate catalysis by triggering the departure of the substrate diphosphate group with the assistance of 3 Mg^{2+} ions (or sometimes 3 Mn^{2+} ions)[8] to generate a carbocation-pyrophosphate (PP_i) ion pair. The ensuing multi-step cyclization cascade is ultimately quenched by proton elimination or addition of a nucleophile such as water to the final carbocation intermediate. Terpenoid cyclases thus catalyze the most complex reactions in biology, since more than half of the carbon atoms in the substrate typically undergo changes in bonding and/or hybridization during the course of a cyclization cascade.

2-Methylisoborneol synthase (MIBS) from *Streptomyces coelicolor* A3(2) is highly unusual among the greater family of class I terpenoid cyclases in that it utilizes the noncanonical, C_{11} substrate 2-methylgeranyl diphosphate (Figure 1).[9–11] This methylated monoterpene is generated from geranyl diphosphate and *S*-adenosyl-L-methionine in a reaction catalyzed by geranyl diphosphate *C*-methyltransferase, encoded by the second gene in the MIBS biosynthetic operon. While MIBS was the first terpenoid cyclase to be discovered that utilizes a noncanonical but naturally-occurring methylated isoprenoid substrate, the subsequent discovery of MIBS in other species of bacteria, as well as the discovery of the related cyclase 2-methylenebornane synthase in *Pseudomonas fluorescens* PfO-1 and *Micromonospora olivatsterospora*, suggests a common role for 2-methylgeranyl diphosphate as a noncanonical isoprenoid substrate for terpenoid biosynthesis.[12–14]

While 2-methylgeranyl diphosphate is a naturally-occurring noncanonical terpenoid cyclase substrate, synthetic non-naturally-occurring analogues of noncanonical terpenoid cyclase substrates, such as fluorinated isoprenoid diphosphates, have been previously described. For example, aristolochene synthase catalyzes the cyclization of 2-fluorofarnesyl diphosphate, 6-fluorofarnesyl diphosphate, and 14-fluorofarnesyl diphosphate into the corresponding fluorinated analogues of germacrene A.[15,16] Substitution of fluorine in the isoprenoid substrate can inductively destabilize carbocation intermediates and their intervening transition states. Accordingly, depending on the site of fluorine substitution and the degree to which positive charge accumulates on a nearby carbon atom during catalysis, a noncanonical fluorinated substrate analogue can be completely unreactive, partially reactive, or fully reactive. Understanding structure-activity relationships in such noncanonical substrates will set an important foundation for developing new strategies for engineering and expanding the substrate specificity of terpenoid cyclases.

We recently reported the X-ray crystal structure of MIBS complexed with the unreactive noncanonical substrate analogue 2-fluorogeranyl diphosphate (2FGPP).[17] The structure of this complex revealed the binding of 2 Mg^{2+} ions coordinated by characteristic metal-binding motifs on the protein and the diphosphate group of the substrate analogue. Although the structure of the unliganded enzyme was not available at the time, it was believed that the structure of the MIBS-2FGPP complex revealed an active site conformation that was incompletely closed and hence catalytically incompetent. The fluorine atom at C2 of 2FGPP was believed to attenuate the reactivity of 2FGPP.

Here, we report the X-ray crystal structure of unliganded MIBS, which has allowed the first study of the conformational changes triggered by ligand binding in the enzyme active site. Additionally, we report the structure of MIBS complexed with 2-fluoroneryl diphosphate (2FNPP), the *cis* isomer of 2FGPP, generated during cocrystallization of MIBS with the

tertiary allylic diphosphate 2-fluorolinalyl diphosphate (2FLPP). This unexpected result demonstrates that the enzyme is capable of ionizing and isomerizing 2FLPP, an analogue of the natural 2-methyllinalyl diphosphate intermediate of the MIBS cyclization reaction (Figure 1). In addition, analysis of the products of solution phase incubation of 2FLPP with MIBS indicates that while the majority of 2FLPP is either recovered unreacted or undergoes simple solvolysis to yield 2-fluorolinalool, a small fraction undergoes MIBS-catalyzed cyclization to generate transiently formed 2-fluoroisoborneol, which undergoes rapid elimination of hydrogen fluoride to yield the observed product (1*R*)-(+)-camphor.

EXPERIMENTAL PROCEDURES

Methods

Gas chromatography-mass spectrometry (GC-MS) analyses were performed using a Hewlett-Packard Series 2 GC-MSD instrument (70 eV, electron impact), a 1 mL injection volume and 3 min solvent delay. Non-chiral GC-MS separation conditions used a temperature program of 60 °C for 2 min, a temperature increment of 20 °C min^{-1} to 280 °C, followed by a 2 min hold at 280 °C, and a HP-5MS capillary column (30 m × 0.25 mm, Agilent Technologies). Chiral GC-MS separation conditions used a temperature program of 50 °C for 1 min, a 10 °C min^{-1} increment to 200 °C, followed by a 1 min hold at 200 °C and a CP-ChiralSil-Dex column (25 m × 0.32 mm ID, Varian). Comparison of GC-MS detected compounds to their standards was done using the MassFinder 4.2.1.0 program. NMR spectra were obtained using a Bruker Avance AV300 NMR spectrometer operating at a 300 MHz ^{1}H frequency.

Synthesis of 2-fluorolinalyl diphosphate (2FLPP)

The synthesis of 2-fluorolinalyl diphosphate is shown in Scheme 1. Triethyl-2-fluoro-2-phosphonoacetate was synthesized according to literature procedures[18] and used to synthesize (±)-2-fluorolinalool according to the method of Karp and colleagues.[19] Diphosphorylation to yield (±)-2-fluorolinalyl diphosphate (2FLPP) was achieved using the two-step method of Cane and colleagues.[20] The ^{1}H, ^{31}P and ^{19}F NMR spectra of 2FLPP, which matched those reported in literature,[19] are shown in Figures S1–S3 of the Supporting Information and definitively establish the chemical purity of the sample.

Incubation of MIBS with 2FLPP

2FLPP was incubated with MIBS in 4 mL of buffer [50 mM PIPES (pH 7.0), 10 mM $MgCl_2$, 100 mM NaCl, 5 mM β-mercaptoethanol] with a 4 mL pentane overlay, at 30 °C for 12 hours. The reaction mixture was extracted with 3 × 4 mL of pentane and the combined pentane layer was reduced to 100 μL *in vacuo* (on ice). GC-MS analysis (non-chiral separation conditions) indicated the presence of minor quantities of 2-fluorolinalool, the hydrolyzed product of 2FLPP. A phosphatase solution [4 mL of 0.1 M sodium acetate (pH 5.0), with 12 units of wheat germ acid phosphatase and 8 units of potato apyrase] was then added to the enzymatic reaction to hydrolyze any remaining 2FLPP to 2-fluorolinalool and incubated overnight at 30 °C with a 4 mL pentane overlay. After extraction with 3 × 4 mL of pentane and concentration, GC-MS analysis using an achiral stationary phase showed an increase in the signal intensity of 2-fluorolinalool as well as minor amounts of camphor.

To determine the absolute stereochemistry of the camphor product, the experiment above was repeated using a longer incubation time of 48 hours. Pentane extracts were loaded onto a pipette column with 5 cm of silica gel (equilibrated with pentane) and the enzymatically-produced camphor was eluted with 100% pentane. The fractions containing camphor were collected and reduced *in vacuo* to near dryness at 0° C.

Since homochiral camphor standards (Sigma-Aldrich) were unresolvable by GC-MS using chiral separation conditions, these standards and the camphor product of the incubation of MIBS with 2FLPP were reduced to their corresponding isoborneol stereoisomers by treatment with $LiAlH_4$. To the MIBS-generated camphor sample under a nitrogen atmosphere was added 3 mL of anhydrous diethyl ether and 10 mg of $LiAlH_4$ (0.26 mmol). The reaction mixture was stirred for 30 min at room temperature and then quenched with 10 μL of water, 10 μL of 15% NaOH, and 30 μL of water. The mixture was filtered, dried with $MgSO_4$ and filtered again. The ether extracts were concentrated *in vacuo* at 0° C to 100 μL and analyzed by chiral GC-MS. Enantiomerically-pure camphor standards were reduced similarly, but on a larger scale (100 mg of camphor (0.65 mmol), 120 mg of $LiAlH_4$ (3.16 mmol), and quenched after 30 min at room temperature with 120 μL of water, 120 μL of 15% NaOH, and 360 μL of water). The isoborneol enantiomers were then resolvable by chiral GC-MS.

Crystal structure determinations

A clone of MIBS from *Streptomyces coelicolor* with a 21-residue hexahistidine tag and linker in a pET28a plasmid (Novagen Inc, USA) was expressed using *Escherichia coli* BL21 (DE3) cells (Stratagene Inc.)[9], purified to homogeneity, and utilized for crystallization experiments using the sitting drop vapor diffusion method.[17] For the crystallization of the unliganded form of this full-length MIBS construct, a 1 μL drop of protein solution [10 mg/mL MIBS, 50 mM piperazine-*N*,*N*′-bis(2-ethanesulfonic acid (PIPES) (pH 7.0), 10% glycerol, 2 mM dithiothreitol, 15 mM $MgCl_2$, 10 mM NaCl, 5 mM $Na_4P_2O_7$, 5 mM 2-azabornane[21]] was added to a 1 μL drop of precipitant solution [100 mM bis-Tris (pH 6.5), 25% polyethylene glycol 3350, 200 mM $MgCl_2$] and equilibrated against a 100 μL reservoir of precipitant solution at 4° C. Octahedral crystals appeared within one day and grew to maximal dimensions of 200 μm × 200 μm × 200 μm in 1–2 weeks. Even though 2-azabornane was included in the crystallization conditions, no evidence for ligand binding was observed in the electron density maps, thereby yielding the first structure of unliganded MIBS (*vide infra*). Crystals were flash-cooled after transfer to a cryoprotectant solution consisting of the mother liquor augmented with 10% glycerol.

For the crystallization of the MIBS-2FNPP complex, a 1 μL drop of protein solution containing 2FLPP [10 mg/mL MIBS, 50 mM PIPES (pH 7.0), 10% glycerol, 2 mM dithiothreitol, 12.5 mM $MgCl_2$, 10 mM NaCl, and 2.5 mM 2FLPP] was added to a 1 μL drop of precipitant solution [100 mM bis-Tris (pH 6.5), 25% polyethylene glycol 3350, 200 mM Li_2SO_4] and equilibrated against a 100 μL reservoir of precipitant solution at 4° C. Octahedral crystals appeared within one day and grew to maximal dimensions of 200 μm × 200 μm × 200 μm in 1–2 weeks. Even though the 2FLPP was included in the crystallization buffer, the electron density map revealed the exclusive binding of 2FNPP (*vide infra*). Crystals were flash-cooled after transfer to a cryoprotectant solution consisting of the mother liquor augmented with 10% glycerol.

Crystals of unliganded MIBS and the MIBS-2FNPP complex diffracted X-rays to 1.85 Å and 2.00 Å resolution, respectively, at the National Synchrotron Light Source beamline X25, using incident radiation with $\lambda = 1.100$ Å. Crystals of unliganded MIBS belonged to space group $P4_322$ with unit cell parameters $a = b = 99.4$ Å, $c = 104.8$ Å, $\alpha = \beta = \gamma = 90°$. Crystals of the MIBS-2FNPP complex belonged to space group $P4_322$ with unit cell parameters $a = b = 99.5$ Å, $c = 105.1$ Å, $\alpha = \beta = \gamma = 90°$. Crystals of both complexes were isomorphous with crystals of the MIBS-2FGPP complex.[17] Diffraction data were processed with HKL2000.[22] While these data sets were characterized by high R_{merge} values, the precision indicating merging R-factor, $R_{p.i.m.}$, which reflects the increased accuracy of highly redundant data

sets, was acceptable for all data sets in all shells of data. Data collection and reduction statistics are recorded in Table 1.

The structures were solved by molecular replacement using the atomic coordinates of the MIBS-2FGPP complex less ligand and solvent atoms as a search probe for rotation and translation functions using PHENIX.[23] Initial rigid body refinement, iterative cycles of positional refinement, and refinement of the grouped and individual atomic *B*-factors were performed; manual model rebuilding was achieved with COOT.[24] Water molecules, Mg^{2+} ions, and ligand (if present) were included in later cycles of refinement. A total of 319 and 325 out of 461 total residues are present in the final models of unliganded MIBS and the MIBS-2FNPP complex, respectively. The N-terminal hexahistidine tag, the linker segment, and residues M1-S110 or M1-A115 in the 13-kDa proline-rich N-terminal domain were disordered and are absent in the final models of unliganded MIBS or the MIBS-2FNPP complex, respectively. Additional disordered segments include surface loops E155-Q160 and C199-G206 in unliganded MIBS. Data reduction and refinement statistics are recorded in Table 1; Ramachandran plot statistics were calculated with PROCHECK.[25] Simulated annealing omit maps were calculated with CNS.[26] Protein structure figures were prepared with the graphics program PyMol (http://www.pymol.org) and labeled for publication using PhotoshopCS.

RESULTS

Structure of unliganded MIBS

No evidence for ligand binding is found in the active site of MIBS crystallized in the presence of millimolar concentrations of 2-azabornane, PP_i, and Mg^{2+}. Since 2-azabornane lacks the *N*-methyl group that would make it a more faithful mimic of the 2-methyl-2-bornyl cation intermediate of the MIBS-catalyzed cyclization reaction (Figure 1), the absence of 2-azabornane may be a consequence of enzyme specificity for noncanonical C_{11} isoprenoid substrates. Regardless, this unliganded structure provides the first view of the fully open conformation of the MIBS active site (Figure 2).

As occasionally observed in the structures of other unliganded terpenoid cyclases, certain loops flanking the active site lack well-defined electron density and are likely disordered. In MIBS, these disordered segments are the A-C loop (E155-Q160) and the D-D1 loop (C199-G206). These loops are expected to become ordered upon the binding of substrate and 3 Mg^{2+} ions that typically stabilize the fully closed active site conformation of a terpenoid synthase.[8] However, these loops remain disordered in the complexes of MIBS with 2 Mg^{2+} ions and the unreactive substrate analogues geranyl thiolodiphosphate or 2FGPP (Figure 2).[17] Accordingly, the structures of these complexes were judged to reflect an incompletely closed MIBS active site that, upon the binding of a third Mg^{2+} ion, would become fully closed and initiate catalysis.[17] The root-mean-square (r.m.s.) deviation of 0.42 Å for 310 Cα atoms between the structures of unliganded MIBS and the MIBS-2FGPP complex supports this conclusion, since such r.m.s. deviations usually exceed 1.0 Å when fully open and fully closed terpenoid cyclase conformations are compared. For example, the r.m.s. deviation for 318 Cα atoms is 1.6 Å between the fully open and fully closed conformations of the bacterial sesquiterpene cyclase epi-isozizaene synthase.[27]

Structure of the MIBS-Mg^{2+}_2-2FNPP complex

Surprisingly, crystallization of MIBS in the presence of millimolar concentrations of racemic 2FLPP and Mg^{2+} yields the structure of the complex with 2FNPP stabilized by Mg^{2+}_B and Mg^{2+}_C ions. With thermal B-factors of 30 $Å^2$ and 50 $Å^2$ for Mg^{2+}_B and Mg^{2+}_C ions, respectively, Mg^{2+}_C is possibly bound with less than full occupancy. This feature, plus

the complete lack of Mg^{2+}_A binding, reflects an incompletely formed trinuclear metal cluster, suggesting that the active site is not fully closed. The r.m.s. deviation of 0.52 Å for 309 Cα atoms between the MIBS-Mg^{2+}_2-2FNPP complex and unliganded MIBS similarly suggests incomplete active site closure. Notably, however, active site loops (the A-C loop and the D-D1 loop) disordered in the unliganded enzyme or in previously-reported enzyme-substrate analogue complexes[17] (Figure 2) are more ordered in the MIBS-Mg^{2+}_2-2FNPP complex, although portions of these segments are characterized by somewhat noisy electron density and generally higher thermal B-factors than their flanking segments. Analysis of crystalline enzyme-ligand complexes with aristolochene synthase from *Aspergillus terreus* suggests that the metal ions bind in the sequence Mg^{2+}_B, Mg^{2+}_C, and finally Mg^{2+}_A.[28] Here, we similarly hypothesize that binding of the Mg^{2+}_A ion would complete the formation of a trinuclear metal cluster in MIBS that would ensure complete active site closure and catalysis.

An electron density map showing the binding of 2FNPP in the active site is found in Figure 3. The diphosphate group of 2FNPP coordinates to the Mg^{2+}_B and Mg^{2+}_C ions and the isoprenoid tail is in an extended conformation. The Mg^{2+}_B ion is coordinated in octahedral fashion by the "NSE" metal-binding motif on helix H (N345, S349, and E353), 2 diphosphate oxygen atoms of 2FNPP, and a water molecule; the Mg^{2+}_C ion is coordinated in octahedral fashion by the carboxylate group of D197, a single diphosphate oxygen atom of 2FNPP, and 4 water molecules. D197 is the first aspartate in the aspartate-rich metal-binding motif DDXXD, which has diverged to DDCYCED in MIBS. The fluorine atom of 2FNPP is 3.3 Å away from R300, which may reflect a weakly polar interaction. Also of note, the plane of the 2,3-allylic double bond is above and approximately parallel to the plane of the aromatic ring of F305 (Figure 4), which may reflect a possible role for F305 in the stabilization of allylic cation intermediates through cation-π interactions.

It is interesting to note that the ionization of 2FNPP and recombination of the resultant PP_i ion at C3 on the same face of the allylic plane would yield the 3*S* isomer of 2FLPP. Possibly, the bound 2FNPP molecule results from the binding, ionization, and isomerization of (3*S*)-2FLPP present in the racemic mixture of 2FLPP used in the cocrystallization experiment. Analysis of the previously-determined structure of the MIBS-2FGPP complex[17] shows that ionization and recombination of PP_i on the same face of the allylic plane would similarly yield (3*S*)-2FLPP. Curiously, however, the conformations of the isoprenoid tails of 2FGPP and 2FNPP differ in these complexes (Figure 4).

Structural comparison of the MIBS-Mg^{2+}_2-2FNPP complex with unliganded MIBS highlights conformational changes that accommodate ligand binding (Figure 5). The A-C loop, helix C, the C-terminal end of helix D, and the D-D1 loop become ordered and/or undergo conformational changes to accommodate ligand binding. In particular, ligand binding induces a kink in helix C and the ordering and repositioning of its N-terminus. This structural change is accompanied by a conformational change of F164, which swings into the active site. Finally, helix J shifts toward the active site and its N-terminus undergoes induced-fit conformational changes to enable hydrogen bonding between R433 and Y434 and the β-phosphate group of 2FNPP. When the active site is in the fully closed conformation, R433 is expected to hydrogen bond with D198, the second residue in the aspartate-rich motif on helix D, based on structural studies of other bacterial and fungal cyclases.[3] However, these residues are separated by more than 5 Å, indicating that the active site remains in a partially open conformation.

Incubation of MIBS with 2FLPP

The identification of 2-fluorolinalool as the major product resulting from incubation of MIBS with 2FLPP for 12 hours (Figure S4) demonstrates that 2FLPP is not significantly

reactive as a MIBS substrate. However, the identification of minor amounts of camphor in the GC-MS analysis (Figure S5) suggests that limited reactivity is nonetheless possible. Specifically, MIBS weakly catalyzes the cyclization of 2FLPP in the same manner as achieved with the biological substrate 2-methylgeranyl diphosphate to yield camphor, which no doubt is formed by rapid elimination of hydrogen fluoride from the initial cyclization product 2-fluoroisoborneol (Figure 6).

Pentane extracts containing MIBS-generated camphor were reduced with $LiAlH_4$ to yield isoborneol, which was then analyzed by chiral GC-MS using chiral separation conditions. A single peak was observed that corresponded to (1*R*)-(−)-isoborneol by direct comparison with an authentic sample (Figures S6–S8). Therefore, (1*R*)-(+)-camphor is the exclusive enantiomer generated in the MIBS-catalyzed cyclization of 2FLPP. This result is consistent with the stereochemistry of the reaction with the native substrate 2-methylgeranyl diphosphate leading to 2-methylisoborneol.

Curiously, 2-fluoronerolol (the product of phosphatase-catalyzed hydrolysis of 2FNPP) is not detected, in contrast with the observation of active site-bound 2FNPP in the crystal structure of MIBS cocrystallized with 2FLPP (Figure 3). Accordingly, we suggest that the formation of enzyme-bound 2FNPP represents a diversion from the cyclization cascade that is sufficiently long-lived and stable to enable crystallization of the enzyme-ligand complex. Since the cyclization product camphor is generated in trace quantities in solution (Figure 6), it is perhaps not surprising that the minor diversion product 2FNPP is not detectable in preparative incubations in solution and indeed may never be released from the crystals.

DISCUSSION

The isomerization of 2FLPP to 2FNPP in the active site of crystalline MIBS was entirely unanticipated. This chemistry nonetheless highlights important aspects of the mechanistic biochemistry of isoprenoid diphosphates. Specifically, the reaction barrier for the acid-catalyzed ionization of a primary allylic diphosphate group, such as that of geranyl diphosphate, is well known to be higher than that for the ionization of a tertiary allylic diphosphate group, such as that of linalyl diphosphate.[29,30] For example, consider that the rate-determining chemical step of the trichodiene synthase reaction is the ionization of the primary allylic diphosphate group of the substrate farnesyl diphosphate and not the ionization of the tertiary allylic diphosphate group of the reaction intermediate nerolidyl diphosphate.[20]

The enhanced reactivity of a tertiary allylic diphosphate similarly applies to the corresponding 2-fluoro derivatives, such that 2FLPP is more reactive than either 2FGPP or 2FNPP. When MIBS is cocrystallized with the primary allylic diphosphate 2FGPP and Mg^{2+}, the structure of the MIBS-Mg^{2+}_2-2FGPP complex reveals the presence of intact and unreacted active site-bound 2FGPP. On the other hand, when MIBS is cocrystallized with the tertiary allylic diphosphate 2FLPP, the structure of the resulting MIBS-Mg^{2+}_2-2FNPP complex indicates that 2FLPP is sufficiently reactive to undergo MIB-catalyzed ionization and allylic rearrangement to yield the enzyme-bound primary *cis*-allylic diphosphate, 2FNPP, which is sufficiently more thermodynamically stable than the bound tertiary allylic precursor, 2FLPP, that only the MIBS-2FNPP complex is observed in the crystalline complex.

At first glance, it is puzzling as to why enzyme-bound 2FNPP does not undergo further cyclization in the active site of MIBS. Reionization would yield the cisoid conformation of the allylic cation which could then be poised for C1–C6 bond formation. However, the full complement of three metal ions typically observed in the fully closed terpenoid synthase

active site[8] is not observed in the active site of crystalline MIBS complexes. Consequently, the enzyme active site is only partially closed. Even so, based on the 2FLPP-2FNPP isomerization chemistry observed in the crystalline MIBS active site, coordination interactions with only two metal ions may be sufficient to trigger the ionization of 2FLPP; recombination of the resultant allylic cation-PP_i anion pair subsequently yields 2FNPP.

Presumably, crystal packing interactions hinder the binding of the third Mg^{2+} ion and the structural transition to a fully closed active site conformation. While two Mg^{2+} ions appear to be sufficient to trigger the ionization of more-reactive 2FLPP in crystalline MIBS, two Mg^{2+} ions are insufficient to stabilize the enzyme-substrate conformation required for cyclization. If the expected full complement of 3 Mg^{2+} ions were bound, we expect that the MIBS active site would adopt a fully closed conformation that would enable cyclization of 2FGPP or 2FLPP to 2-fluoroisoborneol, which would then directly decompose with loss of HF to generate (1*R*)-(+)camphor. The generation of 2-fluoroisoborneol (and thence (1*R*)-(+)-camphor) is in fact catalyzed by MIBS in solution, where there are no crystal lattice constraints to hinder conformational changes required to adopt a fully closed active site conformation. We did not measure the rate of this reaction, however, because very little (1*R*)-(+)-camphor is generated relative to the significant amount of 2-fluorolinalool detected by GC-MS. That 2FNPP is not detected in solution suggests that the observation of this species bound to crystalline MIBS is a consequence of the protein being locked in an incompletely closed, intermediate active site conformation with only two Mg^{2+} ions bound.

Intriguingly, analysis of the bound conformation of 2FNPP in the MIBS active site indicates that, were 2FNPP were to undergo ionization to yield an allylic cation-PP_i anion pair, the PP_i anion would recombine on the same face of the allylic π system to form (*S*)-2FLPP. This is notable, since (*R*)-2-methyllinalyl diphosphate is the postulated intermediate in the natural MIBS-catalyzed cyclization of 2-methylgeranyl diphosphate.[9,10] Possibly, MIBS incubation with the “incorrect” stereoisomer of 2FLPP actually facilitated crystallization. Alternatively, could MIBS utilize this stereoisomer in catalysis? As precedent for such chemistry, (+)- and (−)-bornyl diphosphate synthases can cyclize either stereoisomer of linalyl diphosphate to generate the corresponding stereoisomers of bornyl diphosphate.[31] Similarly, (+)- and (−)-pinene synthases can utilize either stereoisomer of linalyl diphosphate to generate the corresponding enantiomers of pinene.[32] However, the fact that racemic 2FLPP yields only (1*R*)-(+)-camphor as the sole cyclic product when incubated with MIBS suggests that MIBS achieves a productive cyclization geometry only with (*R*)-2FLPP.

In conclusion, the unexpected reactivity of the tertiary allylic diphosphate 2FLPP as it undergoes isomerization to 2FNPP in the active site of crystalline MIBS shows that the tertiary allylic diphosphate form is more reactive than either the cis or trans primary allylic diphosphate isomers of the acyclic monoterpene substrate. Moreover, the structure of the MIBS-Mg^{2+}_2-2FNPP complex reveals new mechanistic insight into stereochemical discrimination during the cyclization reaction. Specifically, structure-mechanism relationships suggest that the active site can accommodate either (*R*)-2FLPP or (S)-2FLPP when 2 Mg^{2+} ions are bound. Regardless, the ionization of 2FLPP in the MIBS-catalyzed cyclization reaction leads solely to the (4*R*)-α-2-fluoroterpinyl carbocation intermediate, based on the formation of the single cyclic product (1*R*)-(+)-camphor. Three Mg^{2+} ions are presumed to be required for the cyclization reaction; it is likely that the binding of a third Mg^{2+} ion and full active site closure compresses the active site contour so as to enforce the binding of (*R*)-2-FLPP, and to enforce the formation of (*R*)-2-methyllinalyl diphosphate during catalysis. Future studies will continue to probe the diversity of substrate discrimination and reactivity in cyclization reactions catalyzed by MIBS using modified monoterpene substrates.

Supplementary Material

Refer to Web version on PubMed Central for supplementary material.

Acknowledgments

Funding

Supported by US National Institutes of Health Grants GM56838 (D.W.C.) and GM30301 (D.E.C).

We thank the National Synchrotron Light Source at Brookhaven National Laboratory for access to beamline X25.

ABBREVIATIONS

2FGPP	2-fluorogeranyl diphosphate
2FGPP	2-fluorogeranyl diphosphate
2FLPP	2-fluorolinalyl diphosphate
2FNPP	2-fluoroneryl diphosphate
GC-MS	gas chromatography-mass spectrometry
MIBS	2-methylisoborneol synthase
PP_i	inorganic pyrophosphate
r.m.s	root-mean-squared

References

1. Davis EM, Croteau R. Cyclization enzymes in the biosynthesis of monoterpenes, sesquiterpenes, and diterpenes. Top in Curr Chem. 2000; 209:53–95.
2. Wendt KU, Schulz GE, Corey EJ, Liu DR. Enzyme mechanisms for polycyclic triterpene formation. Angew Chem Int Ed. 2000; 39:2812–2833.
3. Christianson DW. Structural biology and chemistry of the terpenoid cyclases. Chem Rev. 2006; 106:3412–3442. [PubMed: 16895335]
4. Christianson DW. Unearthing the roots of the terpenome. Curr Op Chem Biol. 2008; 12:141–150.
5. Allemann RK. Chemical wizardry? The generation of chemical diversity in terpenoid biosynthesis. Pure Appl Chem. 2008; 80:1791–1798.
6. Cane DE, Ikeda H. Exploration and mining of the bacterial terpenome. Acc Chem Res. 2011; 45:463–472. [PubMed: 22039990]
7. Wendt KU, Schulz GE. Isoprenoid biosynthesis: manifold chemistry catalyzed by similar chemistry. Structure. 1998; 6:127–133. [PubMed: 9519404]
8. Aaron JA, Christianson DW. Trinuclear metal clusters in catalysis by terpenoid synthases. Pure Appl Chem. 2010; 82:1585–1597. [PubMed: 21562622]
9. Wang CM, Cane DE. Biochemistry and molecular genetics of the biosynthesis of the earthy odorant methylisoborneol in *Streptomyces coelicolor*. J Am Chem Soc. 2008; 130:8908–8909. [PubMed: 18563898]
10. Komatsu M, Tsuda M, Omura S, Oikawa H, Ikeda H. Identification and functional analysis of genes controlling biosynthesis of 2-methylisoborneol. Proc Natl Acad Sci USA. 2008; 105:7422–7427. [PubMed: 18492804]
11. Köksal M, Chou WKW, Cane DE, Christianson DW. Structure of geranyl diphosphate *C*-methyltransferase from *Streptomyces coelicolor* and implications for the mechanism of isoprenoid modification. Biochemistry. 2012; 51:3003–3010. [PubMed: 22455498]

12. Chou WK, Ikeda H, Cane DE. Cloning and characterization of Pfl_1841, a 2-methylenebornane synthase in *Pseudomonas fluorescens* PfO-1. Tetrahedron. 2011; 67:6627–6632. [PubMed: 21804650]

13. Giglio S, Chou WK, Ikeda H, Cane DE, Monis PT. Biosynthesis of 2-methylisoborneol in cyanobacteria. Environ Sci Technol. 2011; 45:992–998. [PubMed: 21174459]

14. Wang Z, Xu Y, Shao J, Wang J, Li R. Genes associated with 2-methylisoborneol biosynthesis in cyanobacteria: isolation, characterization, and expression in response to light. PLoS ONE. 2011; 6:e18665. [PubMed: 21490938]

15. Miller DJ, Yu F, Allemann RK. Aristolochene synthase-catalyzed cyclization of 2-fluorofarnesyl-diphosphate to 2-fluorogermacrene A. ChemBioChem. 2007; 8:1819–1825. [PubMed: 17683054]

16. Miller DJ, Yu F, Knight DW, Allemann RK. 6- and 14-Fluoro farnesyl diphosphate: mechanistic probes for the reaction catalysed by aristolochene synthase. Org Biomol Chem. 2009; 7:962–975. [PubMed: 19225680]

17. Köksal M, Chou WKW, Cane DE, Christianson DW. Structure of 2-methylisoborneol synthase from *Streptomyces coelicolor* and implications for the cyclization of a noncanonical *C*-methylated monoterpenoid substrate. Biochemistry. 2012; 51:3011–3020. [PubMed: 22455514]

18. Köksal M, Jin Y, Coates RM, Croteau R, Christianson DW. Taxadiene synthase structure and evolution of modular architecture in terpene biosynthesis. Nature. 2011; 469:116–120. [PubMed: 21160477]

19. Karp F, Zhao Y, Santhamma B, Assink B, Coates RM, Croteau RB. Inhibition of monoterpene cyclases by inert analogues of geranyl diphosphate and linalyl diphosphate. Arch Biochem Biophys. 2007; 468:140–146. [PubMed: 17949678]

20. Cane DE, Chiu HT, Liang PH, Anderson KS. Pre-steady state kinetic analysis of the trichodiene synthase reaction pathway. Biochemistry. 1997; 36:8332–8339. [PubMed: 9204880]

21. Whittington DA, Wise ML, Urbansky M, Coates RM, Croteau RB, Christianson DW. Bornyl diphosphate synthase: structure and strategy for carbocation manipulation by a terpenoid cyclase. Proc Natl Acad Sci USA. 2002; 99:15375–15380. [PubMed: 12432096]

22. Otwinowski Z, Minor W. Processing of X-ray diffraction data collected in oscillation mode. Methods Enzymol. 1997; 276:307–326.

23. Adams PD, Afonine PV, Bunkóczi G, Chen VB, Davis IW, Echols N, Headd JJ, Hung LW, Kapral GJ, Grosse-Kunstleve RW, McCoy AJ, Moriarty NW, Oeffner R, Read RJ, Richardson DC, Richardson JS, Terwilliger TC, Zwart PH. PHENIX: a comprehensive Python-based system for macromolecular structure solution. Acta Crystallogr. 2010; D66:213–221.

24. Emsley P, Lohkamp B, Scott WG, Cowtan K. Features and development of Coot. Acta Crystallogr. 2010; D66:486–501.

25. Laskowski RA, MacArthur MW, Moss DS, Thornton JM. PROCHECK: A program to check the stereochemical quality of protein structures. J Appl Cryst. 1993; 26:283–291.

26. Brünger AT, Adams PD, Clore GM, DeLano WL, Gros P, Grosse-Kunstleve RW, Jiang JS, Kuszewski J, Nilges M, Pannu NS, Read RJ, Rice LM, Simonson T, Warren GL. Crystallography & NMR System: A new software suite for macromolecular structure determination. Acta Crystallogr. 1998; D54:905–921.

27. Aaron JA, Lin X, Cane DE, Christianson DW. Structure of epi-isozizaene synthase from *Streptomyces coelicolor* A3(2), a platform for new terpenoid cyclization templates. Biochemistry. 2010; 49:1787–1797. [PubMed: 20131801]

28. Shishova EY, Yu F, Miller DJ, Faraldos JA, Zhao Y, Coates RM, Allemann RK, Cane DE, Christianson DW. X-ray crystallographic studies of substrate binding to aristolochene synthase suggest a metal ion binding sequence for catalysis. J Biol Chem. 2008; 283:15431–15439. [PubMed: 18385128]

29. Rittersdorf W, Cramer F. Die Hydrolyse von Phosphaten und Pyrophosphaten Einiger Monoterpenalkohole. Tetrahedron. 1967; 23:3015–3022.

30. George-Nascimento C, Pont-Lezicka R, Cori O. Nonenzymic formation of nerolidol from farnesyl pyrophosphate in the presence of bivalent cations. Biochem Biophys Res Commun. 1971; 45:119–124. [PubMed: 4334520]

31. Croteau R, Satterwhite DM, Cane DE, Chang CC. Biosynthesis of monoterpenes: enantioselectivity in the enzymatic cyclization of (+)- and (−)-linalyl pyrophosphate to (+)- and (−)-bornyl pyrophosphate. J Biol Chem. 1986; 261:13438–13445. [PubMed: 3759972]

32. Croteau R, Satterwhite DM, Cane DE, Chang CC. Biosynthesis of monoterpenes: enantioselectivity in the enzymatic cyclization of (+)- and (−)-linalyl pyrophosphate to (+)- and (−)-pinene and (+)- and (−)-camphene. J Biol Chem. 1988; 263:10063–10071. [PubMed: 3392006]

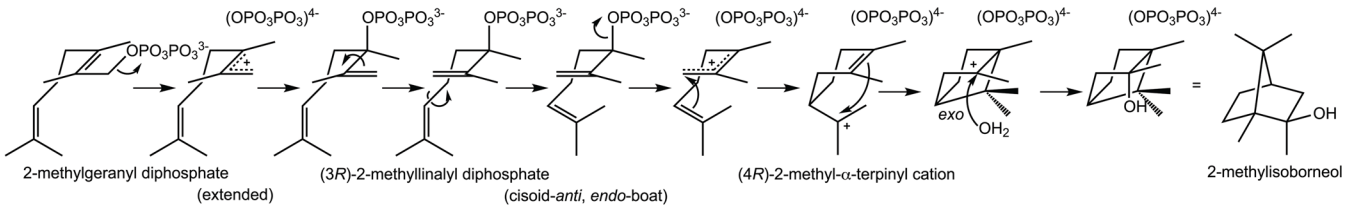

Figure 1.
Proposed cyclization mechanism of MIBS.

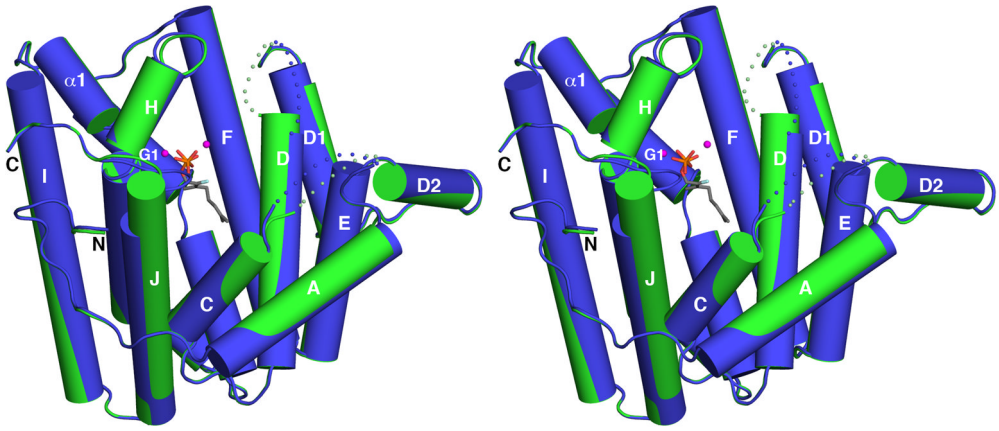

Figure 2.

Superposition of unliganded MIBS (green) with the MIBS-Mg^{2+}_2-2FGPP complex (blue, PDB ID: 3V1X); 2FGPP appears as a stick figure and Mg^{2+} ions are spheres. Dotted lines indicate disordered polypeptide segments. The A-C loop and the D-D1 loop remain disordered in the liganded enzyme, indicating that the enzyme active site in the MIBS-Mg^{2+}_2-2FGPP complex remains in a partially open conformation.

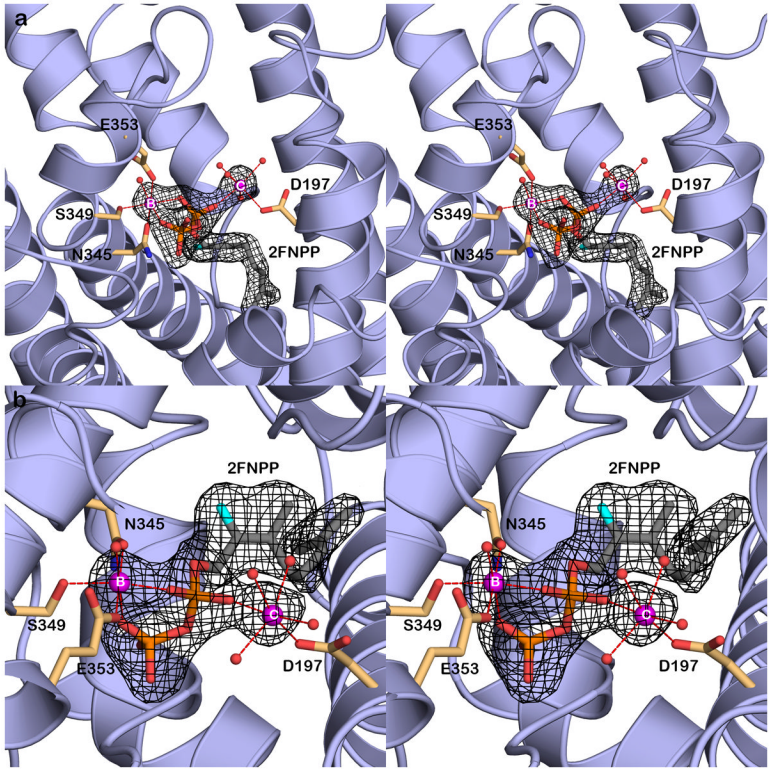

Figure 3.

(a) Simulated annealing omit map of 2FNPP (contoured at 4.0σ) in the MIBS-Mg^{2+}_2-2FNPP complex prepared by cocrystallization of MIBS with 2FLPP. Atoms are color-coded as follows: C = tan (protein) or gray (2FNPP), O = red, N = blue, P = orange, F = cerulean blue, Mg^{2+} ions = magenta spheres, solvent molecules = red spheres. Metal coordination interactions are shown as red dotted lines. (b) Same map as (a), but rotated by ca. 90° and zoomed in to show the cis-isoprenoid linkage of 2FNPP.

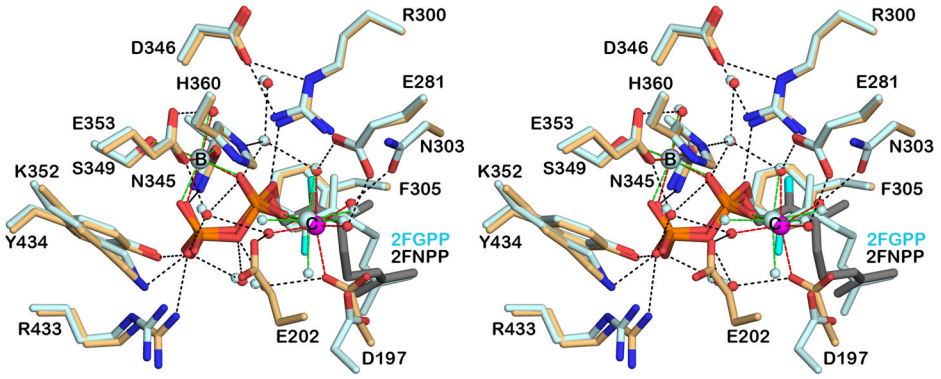

Figure 4.

Superposition of the MIBS-Mg^{2+}_2-2FNPP complex (color-coded as in Figure 3) and the MIBS-Mg^{2+}_2-2FGPP complex (all atoms pale cyan) reveals alternative conformations for the isoprenoid tails of the configurational isomers. Metal coordination and hydrogen bond interactions are shown as red and black dotted lines, respectively.

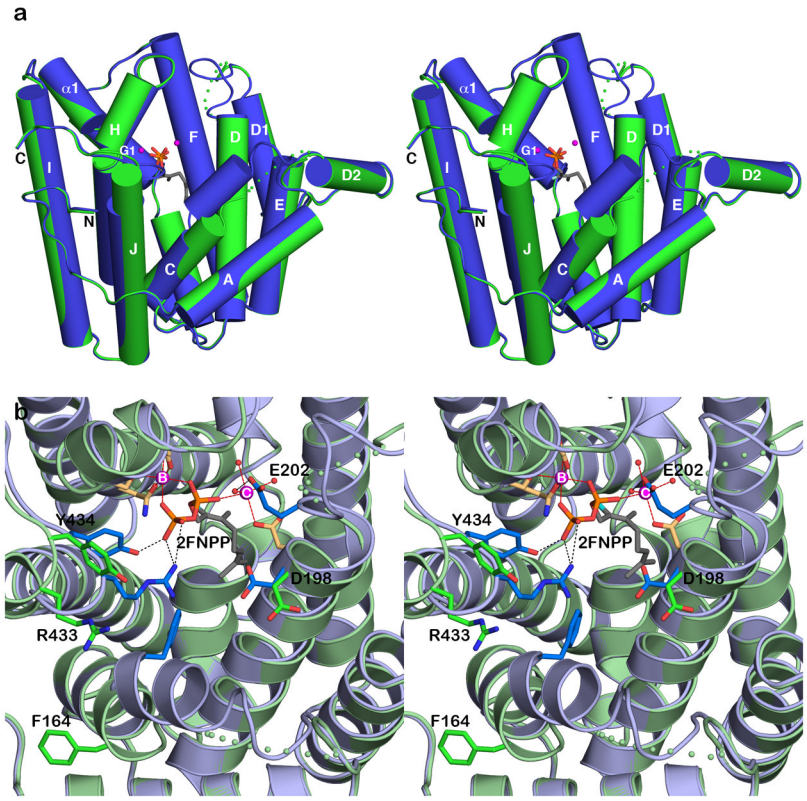

Figure 5.

(a) Superposition of the MIBS-$Mg^{2+}{}_2$-2FNPP complex (blue) and unliganded MIBS (green) reveals conformational changes that occur upon ligand binding. These conformational changes are more extensive that those observed upon the binding of 2FGPP (compare with Figure 2), including the ordering of the A–C loop, helix C (note the significant movement of F164), the D-D1 loop, and the N-terminus of helix J. (b) Close-up view of the superposition of the MIBS-$Mg^{2+}{}_2$-2FNPP complex (light blue ribbon, side chains with blue or tan carbon atoms) and unliganded MIBS (light green ribbon, side chains with green carbon atoms) reveals induced-fit conformational changes that accompany the binding of 2FNPP, $Mg^{2+}{}_B$, and $Mg^{2+}{}_C$. The active site remains partially open in the MIBS-$Mg^{2+}{}_2$-2FNPP complex; in the fully closed conformation, a hydrogen bonded salt link is expected to form between R433 and D198, which in the partially open active site conformation are separated by more than 5 Å.

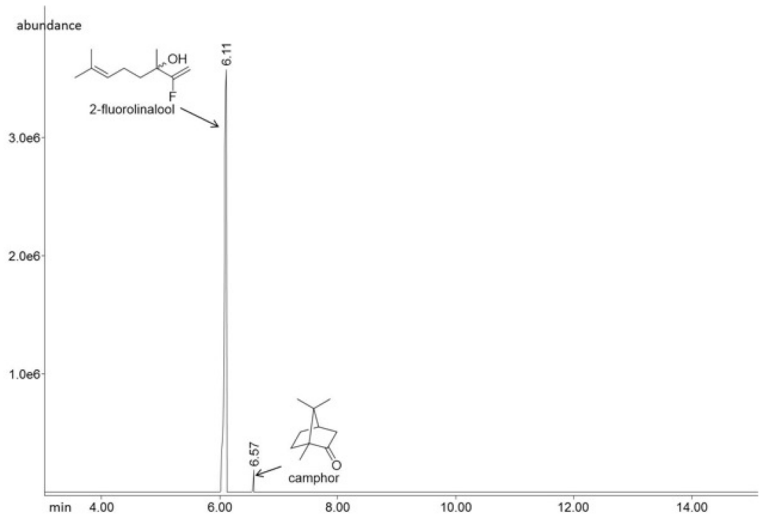

Figure 6.
GC-MS total ion current trace (non-chiral separation conditions) of the pentane extracts from the incubation of 2FLPP with MIBS, followed by incubation with phosphatase solution.

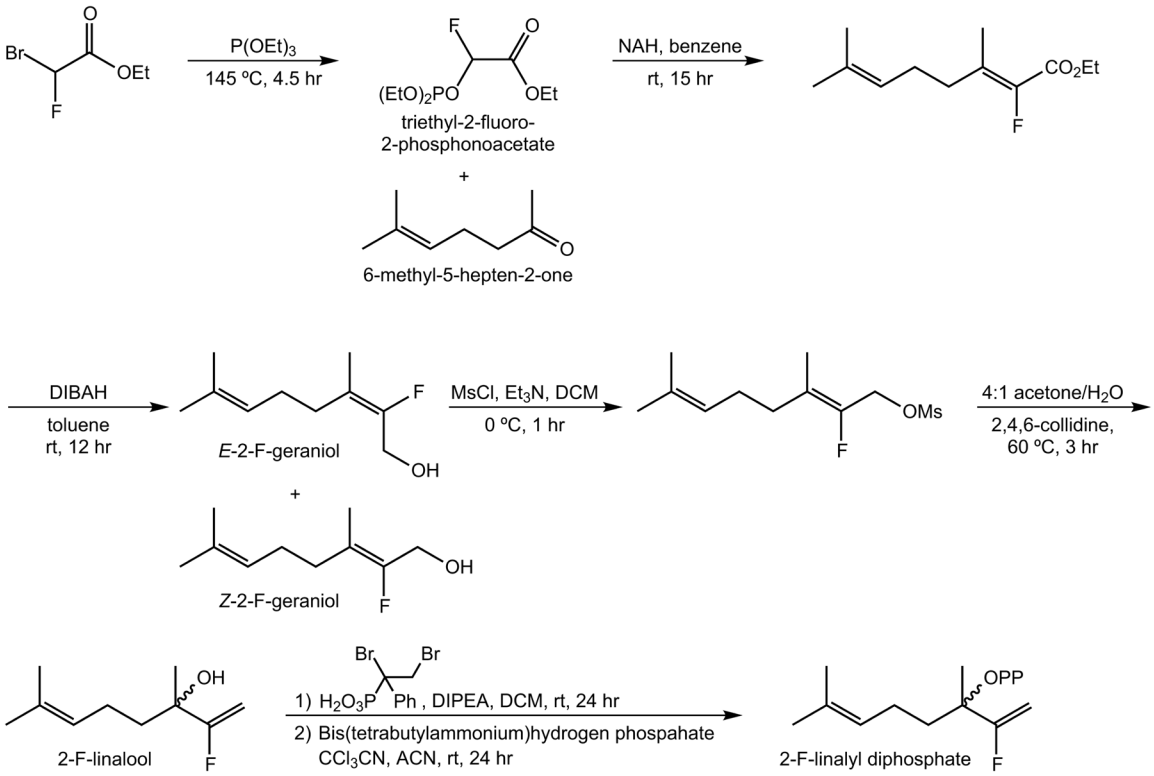

Scheme 1.

Table 1

Data Collection and Refinement Statistics

Structure	Unliganded MIBS	MIBS-Mg_2^+-2FNPP complex
A. *Data Collection*		
Incident wavelength (Å)	1.100	1.100
Resolution range (Å)	50.0-1.85	50.0-2.00
No. of reflections (total/unique)	569,210/45,481	412,445/36,199
Completeness[a] (%)	99.9 (98.7)	100.0 (99.8)
Redundancy[a]	12.5 (11.0)	11.4 (9.7)
I/σ	20.3 (2.1)	12.5 (2.9)
R_{merge}[b]	0.080 (1.168)	0.127 (0.857)
$R_{p.i.m.}$[c]	0.023 (0.360)	0.038 (0.280)
B. *Refinement*		
R_{work}/R_{free} [d]	0.186/0.214	0.173/0.201
Protein atoms[e]	2,534	2,595
Solvent atoms[e]	145	224
2FNPP atoms[e]	0	20
Mg^{2+} ions[e]	0	2
R.m.s. deviations		
Bonds (Å)	0.035	0.008
Angles (°)	2.4	1.1
Dihedral angles (°)	17.9	17.5
Improper dihedral angles (°)	2.6	1.3
Average B factors (Å^2)		
Main chain	35	33
Side chain	38	37
Ligand	-	35
Solvent	35	36
Ramachandran plot		
Allowed (%)	93.7	93.6
Additionally allowed (%)	5.9	6.1
Generously allowed (%)	0.4	0.4
Disallowed (%)	0	0

[a] Number in parentheses refer to the outer shell of data.

[b] $R_{merge} = \Sigma|I-\langle I\rangle|/\Sigma I$, where I is the observed intensity and $\langle I\rangle$ is the average intensity calculated from replicate data.

[c] $R_{p.i.m.} = \Sigma\mathrm{sqrt}(1/n-1)|I-\langle I\rangle|/\Sigma I$, where n is the number of observations (redundancy), I is the observed intensity, and $\langle I\rangle$ is the average intensity calculated from replicate data.

[d] $R_{work} = \Sigma||F_o|-|F_c||/\Sigma|F_o|$ for reflections contained in the working set, and $R_{free} = \Sigma||F_o|-|F_c||/\Sigma|F_o|$ for reflections contained in the test set held aside during refinement (1% of the total number of reflections). and are the observed $|F_o|$ $|F_c|$ and calculated structure factor amplitudes, respectively.

[e] Per asymmetric unit.